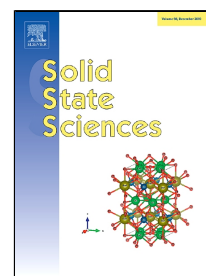


Journal Pre-proof

Ceramic composites for single-layer fuel cells

Piotr Winiarz, Tadeusz Miruszewski, Sebastian Wachowski, Kacper Dzierzgowski,
Iga Szpunar, Krzysztof Zagórski, Aleksandra Mielewczyk-Gryń, Maria Gazda



PII: S1293-2558(19)31053-2
DOI: <https://doi.org/10.1016/j.solidstatesciences.2020.106113>
Reference: SSSCIE 106113
To appear in: *Solid State Sciences*
Received Date: 03 September 2019
Accepted Date: 02 January 2020

Please cite this article as: Piotr Winiarz, Tadeusz Miruszewski, Sebastian Wachowski, Kacper Dzierzgowski, Iga Szpunar, Krzysztof Zagórski, Aleksandra Mielewczyk-Gryń, Maria Gazda, Ceramic composites for single-layer fuel cells, *Solid State Sciences* (2020), <https://doi.org/10.1016/j.solidstatesciences.2020.106113>

This is a PDF file of an article that has undergone enhancements after acceptance, such as the addition of a cover page and metadata, and formatting for readability, but it is not yet the definitive version of record. This version will undergo additional copyediting, typesetting and review before it is published in its final form, but we are providing this version to give early visibility of the article. Please note that, during the production process, errors may be discovered which could affect the content, and all legal disclaimers that apply to the journal pertain.

© 2019 Published by Elsevier.

Ceramic composites for single-layer fuel cells

Piotr Winiarz, Tadeusz Miruszewski, Sebastian Wachowski, Kacper Dzierzgowski, Iga Szpunar, Krzysztof Zagórski, Aleksandra Mielewczyk-Gryń, Maria Gazda

*Gdansk University of Technology, Faculty of Applied Physics and Mathematics
Narutowicza 11/12, 80-233 Gdansk, Poland*

e-mail: piotr.winiarz@pg.edu.pl

Abstract

Composite materials consisting of acceptor doped lanthanum orthoniobate electrolyte phase ($\text{La}_{0.98}\text{Ca}_{0.02}\text{NbO}_4$) and $\text{Li}_2\text{O}:\text{NiO}:\text{ZnO}$ semiconducting phase were synthesized. The precursor powder of $\text{La}_{0.98}\text{Ca}_{0.02}\text{NbO}_4$ was prepared in nanocrystalline (mechanosynthesis) and microcrystalline (solid-state synthesis) form. The composite can be applied in a single-layer fuel cell, because of the presence of two phases acting as an anode and a cathode simultaneously. X-ray diffraction data show that the materials consist of two expected phases. Scanning Electron Microscope images, with Energy Dispersive X-Ray analysis show that $\text{La}_{0.98}\text{Ca}_{0.02}\text{NbO}_4$ as well as $\text{Li}_2\text{O}:\text{NiO}:\text{ZnO}$ are mixed together in the volume of the material. Open circuit voltage both for nano- and microcrystalline composite do not exceed 0.8 V. The single-layer fuel cell is degrading upon time and the voltage drop is observed. The processes of ZnO reduction and Zn diffusion and evaporation as responsible for cell degradation are discussed.

Keywords: lanthanum orthoniobate; proton conductors; EIS; single-layer fuel cell, cell degradation



1. Introduction

In the current stage of electrochemical devices development, single-layer fuel cells are both a potential breakthrough and a controversy. They are assembled with the use of mixed ion-electron conducting (MIEC) composite, which functions both as the electrodes and electrolyte. Since 2011 when Bin Zhu et al. first reported the single-layer fuel cell [1], several attempts of constructing such a cell have been undertaken [2–4]. So far, the only well-functioning, with high power density and long-term stability, single-layer fuel cells were built on the basis of the composites of doped ceria and various semiconducting oxides doped with lithium. Our first works showed that such a type of fuel cells may be constructed using a composite consisted of the acceptor-doped barium cerate as a proton conducting electrolyte and a semiconducting Li-Ni-Zn oxide, however, the power density, as well as the stability of the cell, were poor [5,6].

In this work, a composite of calcium-doped lanthanum orthoniobate ($\text{La}_{0.98}\text{Ca}_{0.02}\text{NbO}_4$) and the Li-Ni-Zn oxide as a semiconducting phase for a single-layer fuel cell is described. The influence of the microstructure of the ceramic composite on the fuel cell performance was studied. Lanthanum orthoniobate as a proton-conducting phase of the composite was chosen because of its relatively high proton conductivity, up to $10^{-3} \text{ S} \cdot \text{cm}^{-1}$ at $800 \text{ }^\circ\text{C}$, and very good chemical stability. The doped lanthanum orthoniobate is also well known for its solely protonic conductivity in a broad range of oxygen partial pressures [7–10]. What is also very important, lanthanum orthoniobate may be easily prepared both in a micro- and a nanocrystalline form [11].

2. Experimental

Calcium doped lanthanum orthoniobate ($\text{La}_{0.98}\text{Ca}_{0.02}\text{NbO}_4$) nanocrystalline powder was prepared by mechanosynthesis. Lanthanum oxide (Alfa Aesar, 99.9%, dried at 900°C for 12 h), niobium (V) oxide (Alfa Aesar, 99.9985%) and calcium carbonate (POCH, 99.9%) were used



as reagents. The powders were mixed in an agate mortar and then ball milled for 12 h at 350 rpm. As a result of the milling procedure a nanocrystalline, quasi amorphous $\text{La}_{0.98}\text{Ca}_{0.02}\text{NbO}_4$ oxide was obtained. In order to prepare also the microcrystalline $\text{La}_{0.98}\text{Ca}_{0.02}\text{NbO}_4$ material, the solid-state synthesis method was applied. The stoichiometric amounts of La_2O_3 , Nb_2O_5 , CaCO_3 were mixed together in an agate mortar and pressed to 1 mm thick pellets using uniaxial pressure of 520 MPa. Samples were heated at 1200°C for 8 hours, then ground, repelletized and annealed at 1400°C for 14 h.

The $\text{Li}_2\text{O}:\text{NiO}:\text{ZnO}$ (LNZ) semiconducting phase was prepared by the solid-state synthesis method. Stoichiometric amounts of ZnO , Li_2CO_3 , and $\text{Ni}(\text{NO}_3)_2 \cdot 6\text{H}_2\text{O}$ powders were mixed to give a cation ratio of 0.15:0.45:0.4, ground in an agate mortar and calcined at 800 °C for 2 hours.

In order to prepare the composite, the nanopowder of $\text{La}_{0.98}\text{Ca}_{0.02}\text{NbO}_4$ and LNZ were mixed in the 2:1 weight ratio. The resultant composite was pressed (200 MPa) uniaxially into pellets of 12 mm diameter and approximately 1 mm thickness. The pellets were sintered using two approaches. In the first one, they were heated with a 5 °C min⁻¹ rate and sintered at either 800 °C or 900 °C for 8 hours. In the other approach sintering process consisted of two steps. In the first step, the pellets were heated to the high temperature between 1000 °C and 1400 °C with a 5 °C min⁻¹ heating rate and held for 1 minute at this temperature and in the second step, the specimens were sintered at 900 °C for 2 hours. The second step was preceded with cooling with the 15 °C min⁻¹ rate. The composite of the lanthanum orthoniobate prepared by the solid-state synthesis method and LNZ was prepared in the same way with the temperature of 1200°C.

Structural characterization of the obtained materials was performed by X-ray diffraction (XRD) using an X'Pert Phillips diffractometer with $\text{Cu K}\alpha$ radiation (1.541 Å). The microstructure of powders and sintered pellets were examined by an FEI Quanta FEG 250 scanning electron microscope (SEM) operating in high vacuum mode, with use of the



backscattered-electron (BSED) detector. Energy dispersive X-ray (EDX) analysis was also performed, utilizing an EDAX Apollo-XD. The average particle size was measured by the grain intercept method described elsewhere [12]. Density measurements were performed using the Archimedes technique with kerosene as medium ($\rho=0.8241 \text{ g}\cdot\text{cm}^{-3}$). The theoretical density of the composite was calculated as a weighted average of the densities of the components where the weight was related to the molar ratio between the substituents.

The composite pellet was then mounted on a testing cell and sealed with glass sealing paste [13]. On both sides of the pellets, the golden paste was deposited and heated at 800°C beforehand. Golden wires were then attached as electrical contacts. One side of the pellet was exposed to a humidified mixture of 90% of Ar and 10% H_2 . The other side was exposed to air. For open circuit voltage (OCV) measurements, Gamry Reference 3000 Potentiostat/Galvanostat was used.

3. Results and discussion

3.1. Materials characterization

The X-ray diffractograms obtained for the precursor oxides as well as the $\text{La}_{0.98}\text{Ca}_{0.02}\text{NbO}_4$ -LNZ composites obtained in various conditions are presented in Figs. 1 and 2.

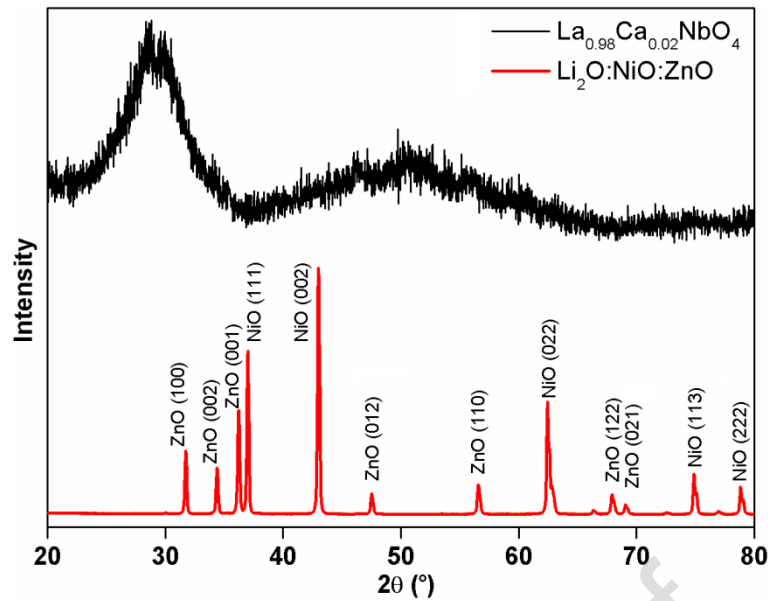


Fig. 1 The diffractograms of the $\text{La}_{0.98}\text{Ca}_{0.02}\text{NbO}_4$ precursor powder after 12h milling and $\text{Li}_2\text{O}:\text{NiO}:\text{ZnO}$ (LNZ) oxide.

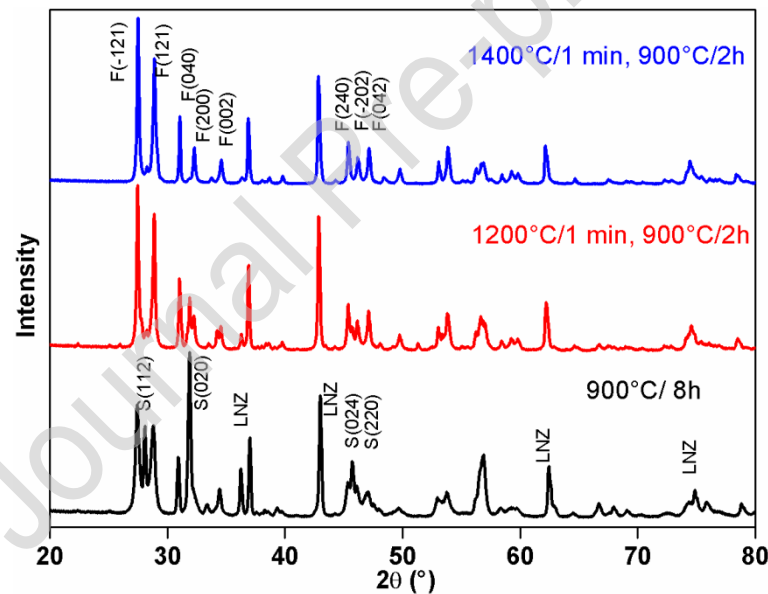


Fig. 2 The diffractograms of $\text{La}_{0.98}\text{Ca}_{0.02}\text{NbO}_4$ – LNZ composites prepared with different heating procedures. Main reflections of fergusonite, scheelite and LNZ phases are marked with F, S and LNZ symbols, respectively.

As can be seen in Fig. 1, the pattern of $\text{La}_{0.98}\text{Ca}_{0.02}\text{NbO}_4$ precursor powder contains a broad maximum at about 30° which is typical of nanocrystalline or quasiamorphous material. The pattern of LNZ shows the reflections of both NiO and ZnO, however there are no XRD reflections of Li_2O . This is related to lithium diffusion into the oxides [6]. Figure 2 shows that

the XRD patterns of the composites prepared with different heating procedures consist of the maxima, which may be attributed to the lanthanum orthoniobate and LNZ semiconducting oxides. The reflections of lanthanum orthoniobate may be indexed mainly within the fergusonite phase (monoclinic, $I2/c$ space group) of LaNbO_4 and also in the scheelite phase (tetragonal, $I4_1/a$ space group). In the $\text{La}_{0.98}\text{Ca}_{0.02}\text{NbO}_4$, fergusonite phase is thermodynamically stable below 500 °C. Around this temperature the phase transition to the tetragonal scheelite phase takes place [14,15]. Figure 2 shows that the application of the first heating step causes the XRD reflections of the scheelite phase disappear. This agrees well with the previous results which showed that stabilization of the tetragonal scheelite phase at room temperature requires either appropriate substitutions [16] or low crystallite size [11]. The maximum temperature at which the crystallites remain small enough for stabilization of the tetragonal crystal structure is 800 °C [11]. Therefore, annealing of nanocrystalline lanthanum orthoniobate at higher temperature inevitably leads to the crystallite growth which subsequently increases the fergusonite-scheelite transition temperature. Figure 2 shows also that the temperature of the first heat-treatment step influences the relative intensities of the reflections of NiO and ZnO in the patterns of the composites. This is caused by the diffusion of Zn into the cubic NiO, whereas the Ni diffusion into ZnO may be neglected [17]. Moreover, no XRD reflections of secondary phases are present in the diffractograms of the composites, which signifies that the components of the composites do not react with one another in the conditions applied for the samples preparation.

The morphology of the composites was imaged by scanning electron microscopy (SEM). The exemplary images of the composite surface prepared with different heating procedures are shown in Figs. 3 and 4. The composite microstructure is typical for polycrystalline ceramic materials, however, it can be seen that the temperature influenced both



the size and shape of the crystal grains. The samples heated at 900 °C, and 1000 °C (Figs. 3a, 3b) are composed of oval grains agglomerated into the larger aggregates.

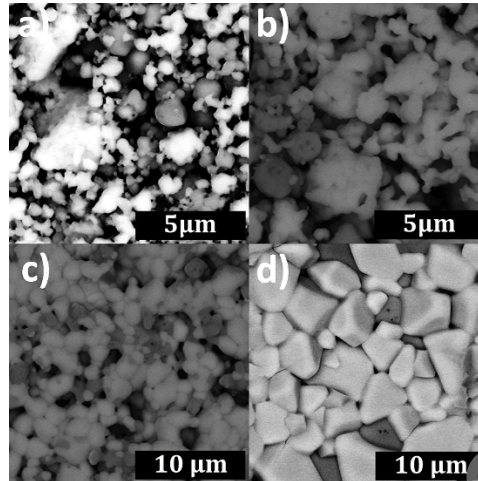


Fig. 3 Scanning electron micrographs of the surfaces of $La_{0.98}Ca_{0.02}NbO_4$ -LNZ composites obtained after process with the first heating step temperatures of a) 900°C, b) 1000°C, c) 1200°C and d) 1400°C.

The average sizes of the grains (Tab.1) are about $(0.9 \pm 0.5) \mu\text{m}$, $(0.8 \pm 0.4) \mu\text{m}$, $(1.7 \pm 0.3) \mu\text{m}$ and $(3.4 \pm 0.3) \mu\text{m}$ in the samples obtained at 900 °C, 1000 °C, 1100 °C and 1200 °C, respectively. For the samples heated at 1000 °C and 1100 °C the grain agglomeration is clearly visible. The morphology of the samples processed at the temperature of 1300 °C and higher (e.g. Fig. 3d) is different. Figures 3 and 4 depict scanning electron micrographs of synthesized composites. It can be seen that the higher temperature of the heat treatment, the less LNZ (dark regions) is present on the surface. The grains are faceted and they are larger, with the average size about $3.7 \mu\text{m}$.

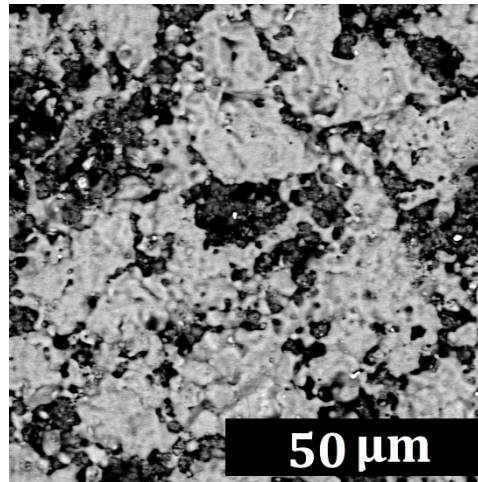


Fig. 4 Scanning electron micrograph of the $La_{0.98}Ca_{0.02}NbO_4$ -LNZ composite surface obtained by solid-state method, performed in the BSE mode.

The surface image of the $La_{0.98}Ca_{0.02}NbO_4$ -LNZ composite obtained with solid-state reaction route is presented in Fig.4. As can be seen, the crystal grains in the sample prepared with this method were larger (3.9 ± 0.4) μm than in the case of the powder prepared with mechanosynthesis.

Tab. 1. Average $La_{0.98}Ca_{0.02}NbO_4$ grain size for different composites

Composite of LNZ and $La_{0.98}Ca_{0.02}NbO_4$	Heating conditions	Average grain size (μm)	Relative density (%)
mechanosynthesis	900 °C /8h	0.9 ± 0.5	57 ± 5
	1000 °C /1 min, 900 °C /2h	0.8 ± 0.4	57 ± 5
	1100 °C /1 min, 900 °C /2h	1.7 ± 0.3	69 ± 5
	1200 °C /1 min, 900 °C /2h	3.4 ± 0.3	76 ± 5
	1300 °C /1 min, 900 °C /2h	3.6 ± 0.4	76 ± 5
	1400 °C /1 min, 900 °C /2h	3.7 ± 0.4	65 ± 5
solid-state synthesis	1200 °C /1 min, 900 °C /2h	3.9 ± 0.4	79 ± 4

To check how these phases are mixed in the volume of the material, the EDX maps were collected and presented in Figure 5. They show that the distribution of both phases in the volume is somewhat more homogenous in the composite prepared using the nanocrystalline $\text{La}_{0.98}\text{Ca}_{0.02}\text{NbO}_4$ precursor powder than in the one obtained with solid-state synthesis. The densities of the pellets fabricated from a mechanosynthesis-prepared precursor strongly depend on the temperature of the first heating step (Tab. 1). The values obtained for the composites heated at 1000 °C and below were relatively low (around 60% of theoretical density). Increasing the temperature of the first heating step leads to obtaining the denser samples. The densities of the composites obtained at 1200 °C and 1300 °C were higher (around 76%). The higher density was found in the case of the composite obtained by the solid-state synthesis and it was equal to 79%. This is consistent with the SEM results, which indicate that the sample prepared by a solid-state synthesis and that heated at 1300 °C contains the least pores.

As all results of microstructural studies indicate, the heating procedure, in particular, the temperature of the first heating step strongly influences the morphology of the material. This step consisted of heating the pellet with a high rate and maintaining the final temperature for one minute after which the sample was quickly cooled down to 900 °C. The aim of this step was to rapidly induce the processes of ceramics densification without causing extensive grain growth [18].

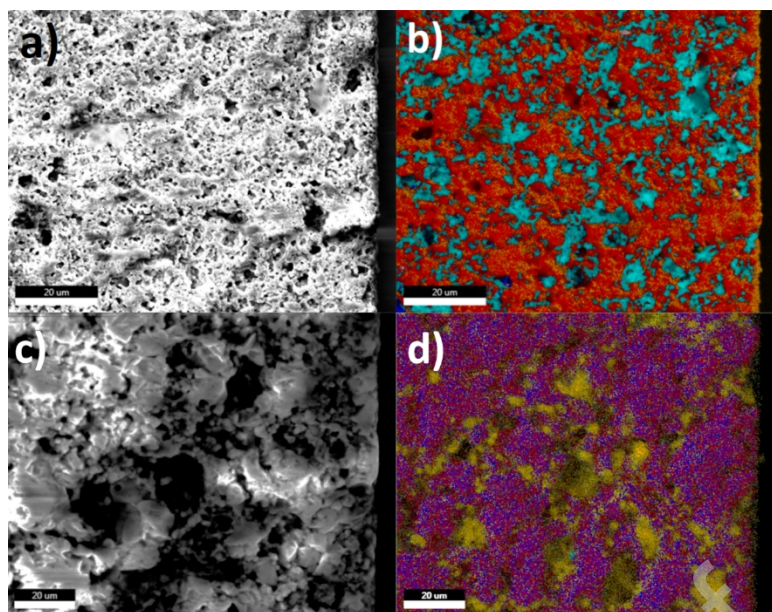


Fig.5 SEM image (a) and the EDX map (b) of the $La_{0.98}Ca_{0.02}NbO_4$ -LNZ composite (1300 °C) fracture (red – $La_{0.98}Ca_{0.02}NbO_4$, cyan – LNZ). SEM image (c) and the EDX map (d) of the $La_{0.98}Ca_{0.02}NbO_4$ -LNZ composite (solid-state synthesis) purple – $La_{0.98}Ca_{0.02}NbO_4$, yellow – LNZ.

As Tab. 1 shows this aim was partially achieved – the density increased from 60% to 76%, however it was accompanied by the grain growth from approximately 1 µm to 3.7 µm. The ceramic composites processed at temperatures below 1200 °C due to their high porosity were not appropriate for functioning as single-layer fuel cells because of high gas leakage through pores. Therefore, for further studies two samples with relatively low porosity and similar grain sizes (the one processed at 1300 °C and the sample obtained by the solid-state synthesis) were chosen.

3.2. Single-layer fuel cell

Time evolution of an open current-voltage (OCV) measured in the single-layer fuel cells constructed on the basis of the $La_{0.98}Ca_{0.02}NbO_4$ – LNZ composites prepared by different methods are presented in Figs. 6a and 6b, respectively. The measurements were carried out in the same atmospheres but at two different temperatures 600 °C (Fig. 6a) and 800 °C (Fig. 6b).

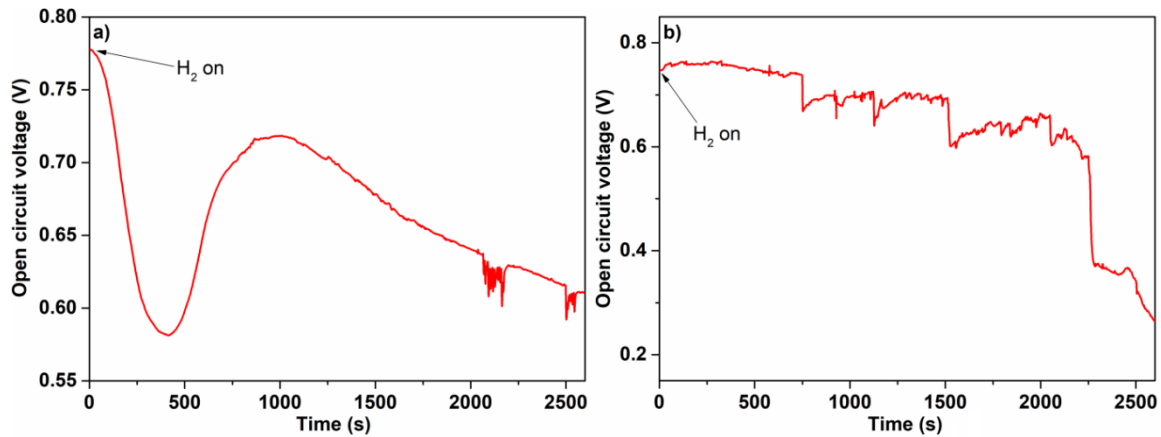


Fig. 6 Open current-voltage (OCV) of the single-layer fuel cell of $La_{0.98}Ca_{0.02}NbO_4$ –LNZ composites: obtained with mechano-synthesis, measured at 600 °C (a), obtained with solid-state synthesis, measured at 800 °C (b).

The OCV measurements were initiated at the moment in which after achieving the thermal equilibrium at final temperature, one side of the pellet was exposed to the Ar/H₂ (90/10) gas mixture. The highest and merely instantaneous noticed OCV was 0.78 V and 0.74 V for the cell-based on composite prepared by mechano-synthesis and solid-state synthesis, respectively. This difference is very small and may be related to the measurement temperature difference as well as microstructure difference, in particular to the total porosity and a pores distribution in the cell. What is the most important, the cells were degrading upon time? The degradation process is much faster at 800 °C. Moreover, at both studied temperatures, the OCV time dependence is not monotonical – it consists of steps in which after a rapid fall, a slower process of increasing OCV may be seen. In order to analyze the reasons for the degradation, the EDX analysis of the pellet after the OCV measurements were performed. The analysis revealed the depletion in Zn in the whole sample (both bulk and surface). We suggest that the mechanism of cell degradation of regions exposed to hydrogen atmosphere occurs as follows: 1) reduction of ZnO into the metallic form of Zn⁰ on the grains surface (this reaction is partially responsible for observed OCV); 2) Zn⁰ evaporation resulting in a rapid decrease of OCV; 3) increase of porosity of the surface regions because of Zn evaporation and subsequent diffusion of reaction gas towards the sample center (slow increase of OCV); 4) processes 1-3 in the interior part of

the pellet accompanied by Zn diffusion towards the surface. Since these processes result in increasing porosity of the composite the final result is the irreversible cell degradation. The processes are much slower if the initial density of the cell is high, as it was seen in [6]. What should be also underlined, during almost the same measurement time (~2500 s) in the case of the cell-based on $\text{La}_{0.98}\text{Ca}_{0.02}\text{NbO}_4$ prepared with the mechanosynthesis (Fig. 6a) only one broad “peak” on OCV curve can be observed whereas in the second cell (Fig. 6b) a large number of smaller and narrower “peaks” was detected. This may be explained by the higher kinetics of the diffusion and evaporation of Zn^0 in the sample related to higher temperature. On the other hand, it is strange that Zhu et al. did not observe degradation in the cells based on ceria and LNZ composite (see in [19]). In such composites both ceria and LNZ may be expected to be reduced in the presence of hydrogen in the atmosphere.

4. Conclusions

Ceramic composites of the acceptor doped lanthanum orthoniobate electrolyte phase ($\text{La}_{0.98}\text{Ca}_{0.02}\text{NbO}_4$) and the $\text{Li}_2\text{O}:\text{NiO}:\text{ZnO}$ semiconducting phase were prepared and studied. The precursor powder of $\text{La}_{0.98}\text{Ca}_{0.02}\text{NbO}_4$ was prepared in nanocrystalline (mechanosynthesis) and microcrystalline (solid-state synthesis) form. The composite phases did not react with another and were homogeneously distributed in the material volume. Different heat-treatment procedures allowed for obtaining the composites of different microstructures. The grain sizes were between 0.9 μm and 3.9 μm , whereas the relative density was between 57% and 79%.

On the basis of the densest composites, single-layer fuel cells were constructed and studied. The highest and merely instantaneous OCV was 0.78 V and 0.74 V for the cell based on the composite prepared by mechanosynthesis and solid-state synthesis, respectively. Generally speaking, the cells degraded quite quickly upon time. The observed OCV time evolution was a sequence of steps in which after a rapid fall, a slower process of increasing



OCV occurred. It was proposed that the ZnO reduction, a diffusion of metallic Zn⁰ and evaporation are responsible for the observed OCV time dependence and the mechanisms of cell degradation.

Acknowledgments:

This work was partially supported by the National Science Centre, Poland [grant number 2015/19/N/ST5/02639]

References

- [1] B. Zhu, R. Raza, G. Abbas, M. Singh, An Electrolyte-Free Fuel Cell Constructed from One Homogenous Layer with Mixed Conductivity, (2011) 2465–2469. doi:10.1002/adfm.201002471.
- [2] B. Zhu, P.D. Lund, R. Raza, Y. Ma, L. Fan, M. Afzal, J. Patakangas, Y. He, Y. Zhao, W. Tan, Q. Huang, J. Zhang, H. Wang, Schottky Junction Effect on High Performance Fuel Cells Based on Nanocomposite Materials, (2015) 1–6. doi:10.1002/aenm.201401895.
- [3] B. Zhu, P. Lund, R. Raza, J. Patakangas, Q. Huang, L. Fan, M. Singh, A new energy conversion technology based on nano-redox and nano-device processes, Nano Energy. 2 (2013) 1179–1185. doi:10.1016/j.nanoen.2013.05.001.
- [4] B. Zhu, Solid oxide fuel cell (SOFC) technical challenges and solutions from nano-aspects, (2009) 1126–1137. doi:10.1002/er.
- [5] K. Zagórski, T. Miruszewski, D. Szymczewska, P. Jasinski, M. Gazda, Synthesis and testing of BCZY / LNZ mixed proton – electron conducting composites for fuel cell applications, Procedia Eng. 98 (2014) 121–128. doi:10.1016/j.proeng.2014.12.498.
- [6] K. Zagórski, S. Wachowski, D. Szymczewska, A. Mielewczyk-Gryń, P. Jasiński, M. Gazda, Performance of a single layer fuel cell based on a mixed proton-electron

- conducting composite, *J. Power Sources*. 353 (2017) 230–236. doi:10.1016/j.jpowsour.2017.04.007.
- [7] R. Haugrud, T. Norby, High-temperature proton conductivity in acceptor-doped LaNbO_4 , *Solid State Ionics*. 177 (2006) 1129–1135. doi:10.1016/j.ssi.2006.05.011.
- [8] S. Wachowski, A. Mielewczyk-Gryń, K. Zagórski, C. Li, P. Jasiński, S.J. Skinner, R. Haugrud, M. Gazda, A. Mielewczyk-Gryn, K. Zagorski, C. Li, P. Jasinski, S.J. Skinner, R. Haugrud, M. Gazda, A. Mielewczyk-Gryń, K. Zagórski, C. Li, P. Jasiński, S.J. Skinner, R. Haugrud, M. Gazda, Influence of Sb-substitution on ionic transport in lanthanum orthoniobates, *J. Mater. Chem. A*. 4 (2016) 11696–11707. doi:10.1039/C6TA03403A.
- [9] M. Huse, T. Norby, R. Haugrud, Effects of A and B site acceptor doping on hydration and proton mobility of LaNbO_4 , *Int. J. Hydrogen Energy*. 37 (2012) 8004–8016. doi:10.1016/j.ijhydene.2011.10.020.
- [10] C. Solís, J.M. Serra, Adjusting the conduction properties of $\text{La}_{0.995}\text{Ca}_{0.005}\text{NbO}_4 - \delta$ by doping for proton conducting fuel cells electrode operation, *Solid State Ionics*. 190 (2011) 38–45. doi:10.1016/j.ssi.2011.03.008.
- [11] T. Miruszewski, P. Winiarz, K. Dzierzgowski, K. Wiciak, K. Zagórski, A. Morawski, A. Mielewczyk-Gryń, S. Wachowski, J. Strychalska-Nowak, M. Sawczak, M. Gazda, Synthesis, microstructure and electrical properties of nanocrystalline calcium doped lanthanum orthoniobate, *J. Solid State Chem.* 270 (2019). doi:10.1016/j.jssc.2018.12.034.
- [12] S. Wachowski, A. Mielewczyk-Gryn, M. Gazda, Effect of isovalent substitution on microstructure and phase transition of $\text{LaNb}_{1-x}\text{M}_x\text{O}_4$ ($\text{M}=\text{Sb}, \text{V}$ or Ta ; $x=0.05$ to 0.3), *J. Solid State Chem.* 219 (2014) 201–209. doi:10.1016/j.jssc.2014.07.041.
- [13] K.M. Dunst, J. Karczewski, T. Miruszewski, B. Kusz, M. Gazda, S. Molin, P. Jasinski,



- Investigation of functional layers of solid oxide fuel cell anodes for synthetic biogas reforming, *Solid State Ionics*. 251 (2013) 70–77. doi:10.1016/j.ssi.2013.03.002.
- [14] C.R. Orthoniobate, Monoclinic-to-Tetragonal Phase Transformation in a, 806 (1997) 0–3.
- [15] R. Haugrud, T. Norby, Proton conduction in rare-earth ortho-niobates and ortho-tantalates, *Nat. Mater.* 5 (2006) 193–196. doi:10.1038/nmat1591.
- [16] A. T. Aldred, S.-K. Chan, M. H. Grimsditch and M. V. Nevitt Displacive Phase Transformation in Vanadium - Substituted Lanthanum Niobate 1983 MRS Meeting. *MRS Proceedings / Volume 24 / 1983*, 24 (1983) 1983.
- [17] H. Kedesdy, A. Drukalsky, X-Ray Diffraction Studies of the Solid State Reaction in the NiO-ZnO System, *J. Am. Chem. Soc.* 76 (1954) 5941–5946. doi:10.1021/ja01652a013.
- [18] X.-H. Wang, I.-W. Chen, Sintering dense nanocrystalline ceramics without final-stage grain growth, *Nature*. 404 (2000) 168–171.
- [19] B. Zhu, H. Qin, R. Raza, Q. Liu, L. Fan, J. Patakangas, P. Lund, A single-component fuel cell reactor, *Int. J. Hydrogen Energy*. 36 (2011) 8536–8541. doi:10.1016/j.ijhydene.2011.04.082.

Piotr Winiarz: Conceptualization, Investigation, Writing - Original Draft, Writing - Review & Editing, Visualization

Tadeusz Miruszewski: Methodology, Writing - Original Draft, Writing - Review & Editing

Sebastian Wachowski: Validation, Writing - Review & Editing

Kacper Dzierzgowski: Writing - Review & Editing

Iga Szpunar: Writing - Review & Editing

Krzysztof Zagórski: Conceptualization, Investigation, Resources, Funding acquisition

Aleksandra Mielewczyk-Gryń: Writing - Original Draft, Writing - Review & Editing

Maria Gazda: Formal analysis, Writing - Original Draft, Writing - Review & Editing, Supervision, Project administration

Journal Pre-proof

Declaration of interests

The authors declare that they have no known competing financial interests or personal relationships that could have appeared to influence the work reported in this paper.

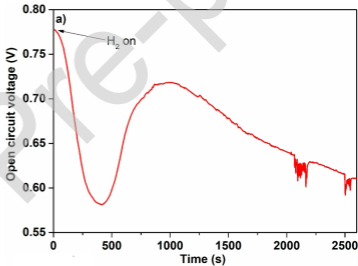
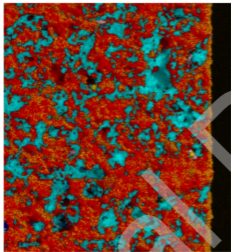
The authors declare the following financial interests/personal relationships which may be considered as potential competing interests:

Journal Pre-proof

- Two-phase synthesized composite material may act as a single-layer fuel cell
- The first heating step influences the morphology of the material
- The open circuit voltage of the composite strongly depends on the microstructure
- Fuel cell degradation upon time may be connected with zinc evaporation

Journal Pre-proof

Single-layer fuel cell



LaNbO_4 and $\text{Li}_2\text{O}:\text{NiO}:\text{ZnO}$ composite

